Modeling X-Ray Propagation Through Beryllium CRLs in the MEC Beamline

Wavefront & aperture aberration simulation as an integrated **PyDM** tool for **Matter in Extreme Conditions** (MEC) hutch; **Graphic User Interface** (GUI) development for beryllium **Compound Refractive Lenses** (CRLs) (Fig. 1).

*Resume

Mateo Brancoli[1,2,*], Dimitri Khaghani[1], Bob Nagler[1]

[1] SLAC National Accelerator Laboratory
[2] Franklin W. Olin College Of Engineering

SLAC NATIONAL ACCELERATOR LABORATORY · U.S. DEPARTMENT of ENERGY · Stanford University · Olin College of Engineering

Beamtime at MEC is scarce, and the CRL configuration that shapes the X-ray beam is still chosen by hand. Among other questions, operators ask: given a photon energy and lens inventory, *how do I prepare the beam to arrive at the Target Chamber Center (TCC) at this spot size and energy density?*

Building the Model (Fig. 2)**.** The MEC acceptance table gives the Full-Width Half Maximum (FWHM) source divergence on a 50-point grid from 800 eV to 25 keV. A single power law fits the whole range to 1.2 % RMS (Fig. 3). Source size is not an input. It is the product of two independent columns, divergence and tabulated virtual-source location, which sits inside the undulator and so adds to the undulator distance. At 8.3 keV this returns 59.9 µm against a published spec of 60 µm, and 2.05 µrad against a spec of 2 µrad.

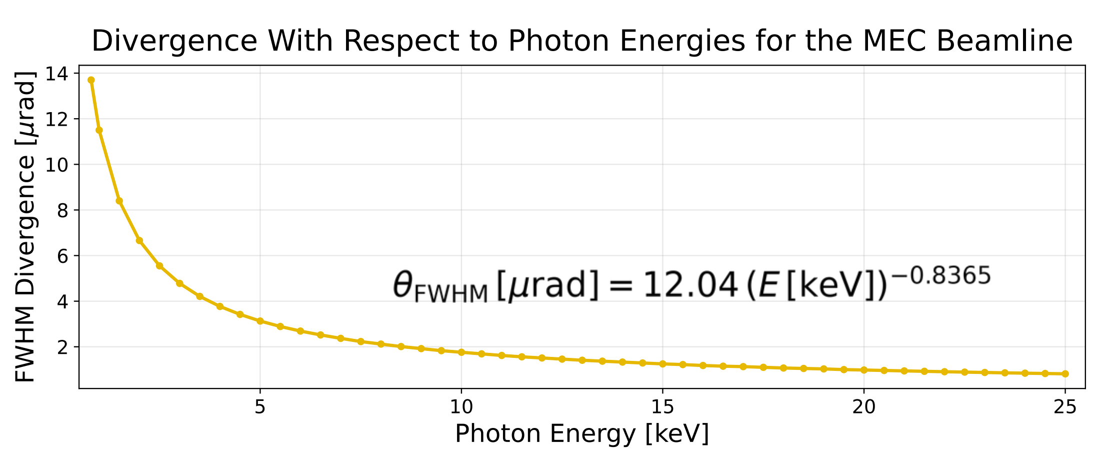

Figure 3. FWHM source divergence for the HXR Cu branch, from the beamline acceptance table.

Tabulated atomic scattering factors fix the refractive index, and with the apex radius the individual lens' focal lengths where δ is the refractive-index decrement, r_e the classical electron radius, λ the wavelength, n_a the atomic number density of the lens material, f_1 the real scattering factor, R the apex radius and f the single-lens focal length: $\delta = \frac{r_e \lambda^2}{2\pi} n_a f_1(E)$ The geometric clear radius of a parabolic lens follows from the same two numbers [8]: $R_0 = \sqrt{R\,(l - d_{\mathrm{web}})}$ where R_0 is the geometric clear radius, l and d_{web} the disk and web thickness

Beam size is computed by marching a marginal ray (h, u) the full 409 m from source to sample where h is the ray height from the axis, u its angle, and $M_1 \dots M_n$ the matrices in beam order, so the rightmost acts first. Free space and a thin lens are the two standard ray-transfer matrices, so a whole cassette is one matrix product. For example, a 12-lens pack is expanded into 12 elements at 1 mm pitch rather than lumped into a single thin lens, so the thick-pack focal shift emerges from the trace instead of being applied afterwards as a correction. The pack integrals factorize exactly into three independent channels: absorption through the flat web, absorption through the parabolic body, and hard truncation at the aperture where T is the fraction of photons through one pack, μ the lens material's attenuation coefficient, σ the incident beam width, and Σ the width after absorption narrows it [1], [8]: $T = e^{-\mu d_{\mathrm{web}}} \cdot \frac{\Sigma^2}{\sigma^2} \cdot \left[1 - e^{-R_0^2/2\Sigma^2}\right]$

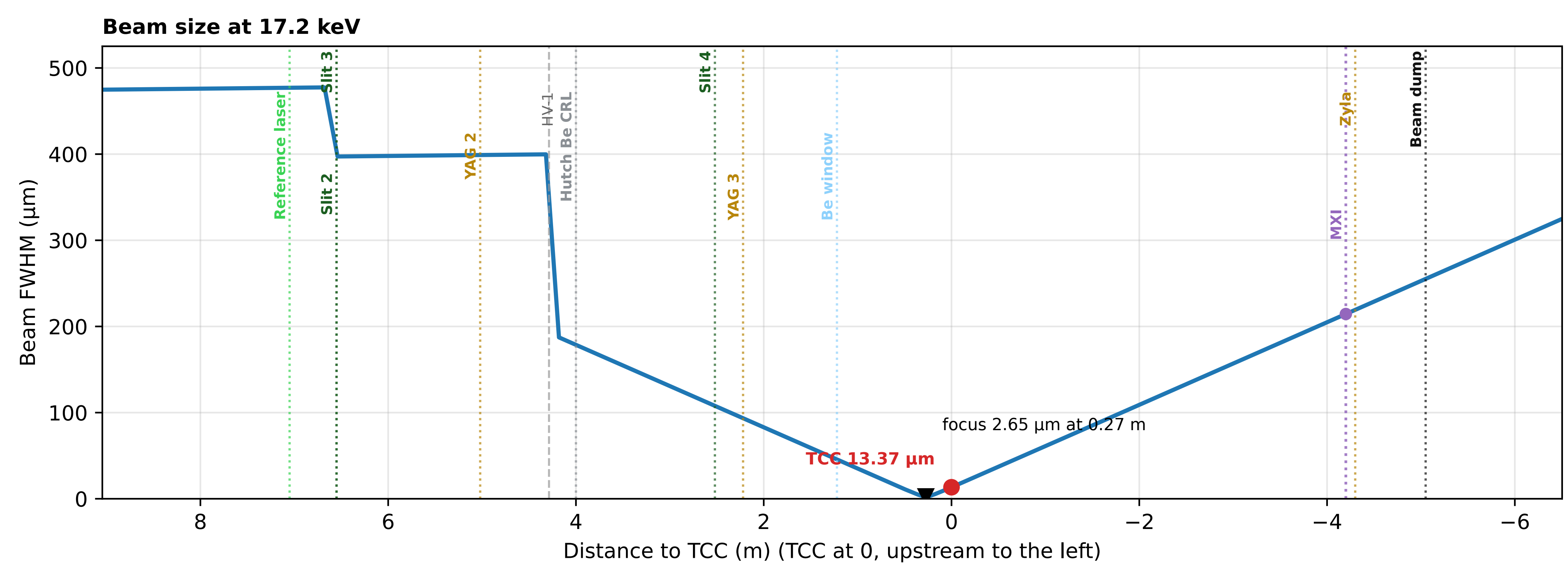

Figure 2. Plot showing the full width half maximum along the beamline with positioners for each instrument and or optic.

The absorption-narrowed width and the stack curvature sum given by $\frac{1}{\Sigma^2} = \frac{1}{\sigma^2} + 2\mu G$ $G = \sum \frac{N_i}{R_i}$, where G is the stack's combined curvature and N_i the lens number of radius R_i. So because the channels separate, the photon budget can say why the flux went, not just how much. For the default 17.2 keV hutch stack the body term dominates so a wider pinhole would not help. Slit jaws are finite slabs with an attenuation length λ_{att}, not perfect absorbers; X-rays are not fully clipped: $T = T_{\mathrm{open}} + T_{\mathrm{jaw}}(1 - T_{\mathrm{open}})$ $T_{\mathrm{jaw}} = e^{-t/\lambda_{\mathrm{att}}}$

An aperture bounds the beam's 95 %-containment radius, not its half-FWHM where d_{95} is the diameter holding 95 % of a Gaussian's power. The coefficient 2.079 is exact; using the half-FWHM instead makes clipping look about twice as gentle as it is: $d_{95} = 2.079 \times \mathrm{FWHM} \;\le\; 2R_0$. Now, the truncated opening then diffracts, and the spread is carried downstream [4]: $\theta_g = 0.443\,\frac{\lambda}{g}$ $\theta_A = 0.514\,\frac{\lambda}{D}$ $u \leftarrow \sqrt{u^2 + \theta^2}$ where θ_g is the sinc² half-angle from a slit of gap g, θ_A the Airy equivalent for a circular aperture of diameter D, and u the ray angle, which the spread adds to in quadrature.

YAG Screen (Fig. 4). Key simulation tool for aberrations.

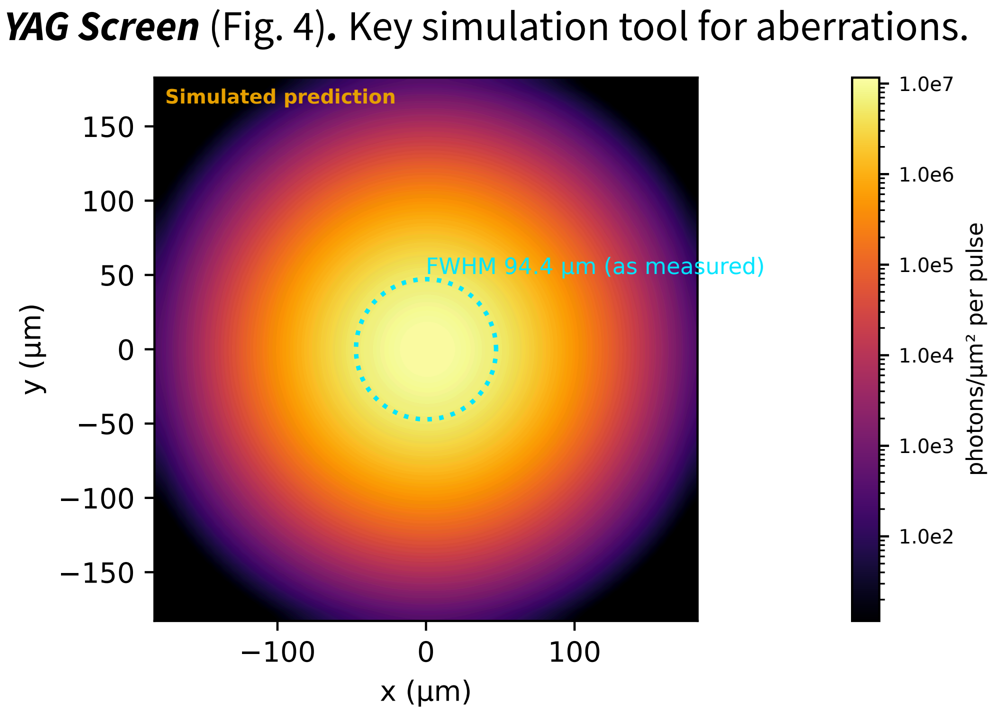

Figure 4. Spatial beam profile at a YAG3 +2.2m on beamline.

Every lens contributes its own complex pupil where T(r) is the complex transmission at radius r, k = 2π/λ the wavenumber, circ(·) the unit disc, and h(r) the surface error (the deviation from an ideal parabola, converted to optical path by δ) [6], [8]: $T(r) = e^{-\mu G r^2/2}\,\mathrm{circ}\!\left(\frac{r}{R_0}\right)\,e^{-ikr^2/2f}\,e^{ik\delta h(r)}$

Propagation between planes is one law, and it carries the same matrix that marched the ray:

$$E_{\mathrm{out}}(r') = \frac{e^{ikL}}{i\lambda B} \iint E_{\mathrm{in}}(r)\,T(r)\,\exp\left\{\frac{ik}{2B}\left[A\,r^2 - 2\,r\cdot r' + D\,r'^2\right]\right\} d^2r$$

$$\text{with} \quad \begin{pmatrix} A & B \\ C & D \end{pmatrix} = M_n \cdots M_2\, M_1$$

where E_{in}, E_{out} are the complex field before and after, r, r' the transverse coordinates in each plane, A, B, C, D the system's ray-transfer matrix elements, and L the on-axis path. For free space A = D = 1, B = L, C = 0, and this reduces to the ordinary Fresnel integral. And this evaluated as a single Fourier transform per hop:

$$E_{\mathrm{out}} \;\propto\; e^{ikDr'^2/2B}\,\mathcal{F}\Big\{E_{\mathrm{in}}\,T\,e^{ikAr^2/2B}\Big\} \qquad \Delta x' = \frac{\lambda B}{M\,\Delta x}$$

where $\mathcal{F}$ is the two-dimensional Fourier transform, Δx the input grid spacing, Δx' the output spacing and M the padded array size. The focal-plane pixel size is set by B and the grid.

Discussion & Future Feature Development. Several features remain to explain, but the GUI will soon be uploaded to GitHub and integrated into MEC devops. On the simulation side: because the pupils multiply, figure error accumulates coherently rather than averaging out, so aberration grows with lens count. Seiboth et al. measured exactly this on beryllium CRLs and corrected it with a refractive phase plate [6]. A stack chosen for focusing power alone therefore pays for it in wavefront quality. The tightest configuration is not always the best one. * Simulated images report this with the Strehl ratio: $\mathcal{S} = \frac{I_{\mathrm{aberr}}(0)}{I_{\mathrm{ideal}}(0)}$ with $I = |E|^2$

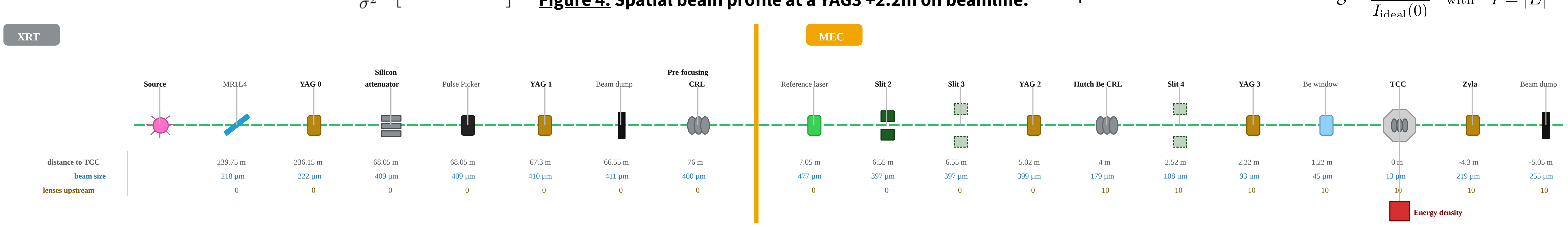

Figure 1. Schematic of the XRT - MEC beamline with respective components; active/clickable components include the attenuator, the Yttrium Argon Garnet (YAG) screens, the CRLs & slits.

References

[1] B. Nagler, "Be Lenses in MEC," technical note, Oct. 3, 2012.
[2] B. Nagler, "Ronchi Testing: Shearing Interferometric Wavefront Sensing and Focus Determination of an XFE," unpublished manuscript, Jul. 8, 2026.
[3] B. Nagler et al., "Focal spot and wavefront sensing of an X-ray free electron laser using Ronchi shearing interferometry," Scientific Reports, vol. 7, Art. no. 13698, 2017.
[4] A. Schropp, "Experimental coherent X-ray diffractive imaging: Capabilities and limitations...," Ph.D. dissertation, Dept. Phys., Universität Hamburg, Germany, 2008.
[5] Y. Liu et al., "X-ray free-electron laser wavefront sensing using the fractional Talbot effect," Journal of Synchrotron Radiation, vol. 27, pp. 254–261, 2020.
[6] F. Seiboth et al., "Perfect X-ray focusing via fitting corrective glasses to aberrated optics," Nature Communications, vol. 8, Art. no. 14623, 2017.
[7] M. Makita et al., "Double grating shearing interferometry for X-ray free-electron laser beams," Optica, vol. 7, no. 5, pp. 404–409, May 2020.
[8] B. Lengeler et al., "Imaging by parabolic refractive lenses in the hard X-ray range," Journal of Synchrotron Radiation, vol. 6, pp. 1153–1167, 1999.

Acknowledgements

Wanted to personally thank members of the **MEC** department for their inclusivity, nurturing moments, and much more; to **Bob Nagler** for assertion and support, to **Dimitri Khaghani** for their championship, to **Nick Czapla** for the bundles of bright energy, to **Hae Ja** for being a true guardian angel, to **Eric Galtier** for being such a magical force of nature, to **Amanda Chen** for the cozy-copilot aura, to **Ariel Arnott** for the heart-felt conversations, and to **Shao Xian Lee** for our spicy occasions.

Use of the Linac Coherent Light Source (LCLS), SLAC National Accelerator Laboratory, is supported by the U.S. Department of Energy, Office of Science, Office of Basic Energy Sciences under Contract No. DE-AC02-76SF00515.